

TWENTYFIFTH EUROPEAN ROTORCRAFT FORUM

Paper n°H8

**A ROTOR VORTEX WAKE MODEL FOR HELICOPTER FLIGHT MECHANICS
AND ITS APPLICATION TO THE PREDICTION OF THE PITCH-UP
PHENOMENON**

BY

**Pierre-Marie BASSET, Ahmed EL OMARI
ONERA, FRANCE**

**SEPTEMBER 14-16, 1999
ROME
ITALY**

**ASSOCIAZIONE INDUSTRIE PER L'AEROSPAZIO, ISISTEMI E LA DIFESA
ASSOCIAZIONE ITALIANA DI AERONAUTICA ED ASTRONAUTICA**

H08

A ROTOR VORTEX WAKE MODEL FOR HELICOPTER FLIGHT MECHANICS AND ITS APPLICATION TO THE PREDICTION OF THE PITCH-UP PHENOMENON

Pierre-Marie BASSET, Ahmed El OMARI

Research Engineer
ONERA

Graduate Student of ENSAE,
Ecole Nationale Supérieure de l'Aéronautique et de l'Espace

Office National d'Études et de Recherches Aéropatiales, ONERA,
Laboratoire ONERA/Ecole de l'Air, BA 701, 13661 Salon-de-Provence, FRANCE

A rotor wake model for helicopter flight mechanics is presented in details. The wake is mainly represented by vortex rings, on which the vorticity distribution is described by Fourier series. The induction formula given in this paper are not limited in harmonics. After the description of the model, the problem of the prediction of the pitch-bump is addressed. The aim is to develop physically based models with a minimum dependence on empiricism, in order to be helpful in the design process of a new helicopter by reducing the number of tests. The effects of the main rotor inflow, of the wake roll-up and of the wake contraction, are studied with analytical models.

NOTATION

a	Longitudinal ½ dimension of elliptic vortex
b	Number of blades, or lateral ½ dimension of elliptic vortex
c	Local blade chord
$(C_t)_{ae}$	Rotor aerodynamic thrust coefficient
C_z	Airfoil lift coefficient
N_h	Number of harmonics
R	Rotor radius
V_{airp}	Airspeed in the airfoil plane
V_z	Vertical speed
$(v_{i0}, v_{i1c}, v_{i1s})$	First harmonic coefficients of the induced velocity field on the main rotor
γ_{ij}	Local vortex strength
$(\gamma_0, \gamma_{1c}, \gamma_{1s})$	First harmonic coefficients of the vorticity distribution on a vortex rings
Γ_{ij}	Local bound circulation on a blade-element
χ	wake skew angle
ψ	Azimuth angle
μ	Advance ratio
Ω	Rotor rotational speed

INTRODUCTION

ONERA contributes to the development of the "Helicopter Overall Simulation Tool" (HOST code) of EUROCOPTER. In the ONERA center of Salon-de-Provence, these mathematical modelling developments are devoted to a better simulation of the helicopter flight dynamics. For rotary wings aircrafts, the modelling of the

rotor wake is very important since its induced velocity field has a significant impact both on the rotor aerodynamics and on the airloads of the other components, in particular the tail elements (horizontal stabilizer, fin and tail rotor).

One of our main goals is to develop a generic rotor wake model which can be applied for trim computations but also for dynamic simulations. The paper will present in details a rotor wake model which can be used routinely for non-real-time simulations including dynamic manoeuvres.

In most helicopter flight mechanics codes, empirical models are used to assess the aerodynamic influences of the main rotor wake on the tail components. But these models requires some experimental data to be tuned and oft, they are not very reliable for the dynamic simulations due to some quasi-steady assumptions.

The vortex method being closer to the physics, provides models with less dependence on empiricism. Therefore the vortex approach has been chosen to obtain a model useful in the design process of any helicopter. Nevertheless, the vortex method is still rarely used in flight dynamics, and among the rare vortex representations applied, the flat vortex wake approximation has been up until now preferred for its low time consuming cost [e.g. 1-4]. But this wake approximation is not valid at low speeds ($\mu < 0.15$), which is precisely the area of the stronger rotor wake interference effects.

On the other hand, more realistic representations, like the free-wake approach [5] or other vortex lattice models [6], have a too high computational cost. That is why their use is still limited to trimmed flight cases.

A compromise has been found with the vortex rings approach [7]. The main rotor wake is represented by : vortex torus distributed along the wake (trailing vortices) with radial vortex segments (shed vortices), (Fig. 1). After a more complete description of the model, its application to the prediction of the aerodynamic interactions will be addressed.

In a previous paper [8], this model has been used to study the wake distortion effects on the inflow field at the main rotor level. The present paper will deal with the main rotor wake influences on the rear components. The study will be focused on the simulation of the pitch-up effect, which is mainly due to the main rotor downwash on the horizontal tail.

Indeed, there is an actual need for a general and reliable model in this area. Still nowadays, the dimensioning of the horizontal stabilizer of a new helicopter requires flight or wind tunnel tests [9].

Several modelling refinements will be presented to improve the simulation of this nose-up behaviour. The effect of a change of main rotor inflow model will be studied. An analytical modelling of the wake roll-up and of the wake contraction will be also evaluated.

ROTOR WAKE MODEL

The rotor wake model is the dynamic vortex rings model described in [7, 10], which has been developed by ONERA especially for the needs of helicopter flight mechanics.

Dynamic vortex rings model

As in any vortex model, the velocity vector induced by the main rotor wake is calculated at any point in space with the Biot and Savart law. This law of induction requires the knowledge of the wake geometry and its vorticity distribution.

WAKE GEOMETRY AND KINEMATICS

* Geometry :

The idea is to represent the complex rotor wake with vortex elements which have a simple prescribed geometry.

The trailing helical vortex lines generated by the gradient of circulation along the blade span, are represented by circular vortices. Indeed, each ring can be viewed as the projection of a helical cycle on the local medium plane normal to the wake axis. Therefore, the more the helical thread (dH) is small, the more the helical line can be approximated by vortex rings distributed along the wake.

In other words, the representation is all the more valid since the number of blades (b) or the rotor speed (Ω) is high, and the normal airspeed through the rotor is low, because :

$$dH(m) = (V_z - v_{i0}) \times \frac{2\pi}{b\Omega}$$

The trailing vortices produced during one rotor revolution are represented by a group of concentric and coplanar vortex rings. Their radii correspond to the radial discretization of the blade, a trailing vortex line being emitted from the root and the tip of the blade and between the blade elements.

In the plan of each group of vortex rings, radial segments are added between two azimuth directions occupied by the blade, in order to model the shed vortices.

Thus, the vortex wake is finally represented by vortex rings with radial vortex segments (Fig. 1). Furthermore, the model is completed by vortex segments distributed along the blade span in order to model the direct effect of each blade element on the airflow by means of bound vortices.



Fig. 1 : Geometry of the rotor wake model.

Viscous core radii are required in order to avoid that the induced velocities take infinite values near a vortex element. A circular vortex is in fact represented by a torus and a segment by a tube.

* Kinematics :

The orientation of each plan of vortices is given by the rotor attitude when they are shed in the wake. Therefore that kind of wake distortions due to the roll and pitch rates of the rotor are taken into account [8].

The initial position of the center of each vortex group corresponds to the position of the rotor center at the time of its generation. Then, each vortex group is convected away from the rotor by the resultant fluid velocity across the rotor at the time of the vortex ring emission. The convection velocity is assumed to be the vector sum of the free stream velocity and the mean downwash velocity (v_{i0}) :

$$\vec{V}_{convec}^{i_{age}} = \vec{V}_{air_{CTR}}(t_{emis}(t_{age})) + \vec{V}_{i0}(t_{emis}(t_{age}))$$

The mean line of the wake is thus representative of the rotor trajectory and of the evolution of the mean aerodynamic load ($v_{i0} = f(C_T)$).

VORTICITY

The vorticity distributions on the rings are approximated by Fourier series. The model presented here is not limited in harmonics. The Fourier's coefficients ($\gamma_0, \gamma_{1c}, \gamma_{1s}, \dots$) for each *vortex ring* are calculated from the local vortex strengths at the radial position corresponding to the considered ring. These local values are computed from the radial gradient of bound circulation ($\partial\Gamma(r, \psi)/\partial r$) on the blades.

The vorticity of each *shed vortex* is calculated from the time derivative of the circulation around the associated blade element. The vorticity of the *bound vortices* is assessed by the circulation around each blade element. The local values ($\Gamma(r, \psi)$) of the bound circulation at the middle of each blade element is calculated according to the Kutta and Joukowski law :

$$\Gamma(r_i, \psi_j) = \frac{c_l}{2} \times V_{air_{r_i, j}} \times C_{z_{i, j}}$$

where (c) is the chord, (V_{air_p}) is the airspeed in the airfoil plane and (C_z) is the local value of the lift coefficient.

The computation of these different vortex intensities are presented schematically on (Fig. 2).

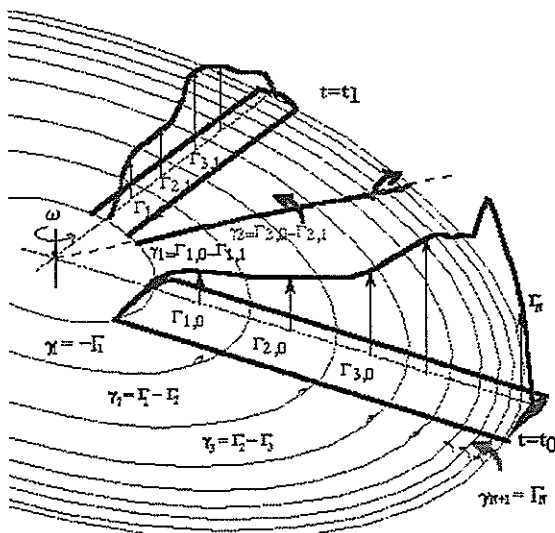


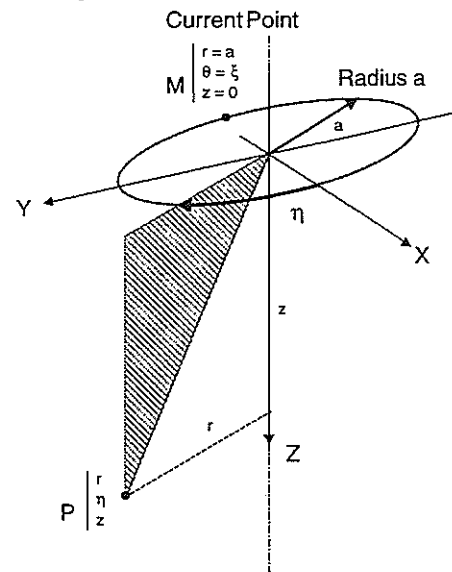
Fig. 2 : Vorticity of the rotor wake model.

3D-INDUCED VELOCITY FIELD BY A CIRCULAR VORTEX

The influence of the wake, defined by its geometry and by its vorticity, is expressed in terms of induced velocities by the Biot and Savart law :

$$\vec{V}_i(P) = -\frac{1}{4\pi} \int \gamma(M) \frac{\vec{MP} \wedge d\vec{l}_M}{|MP|^3}$$

The interest of using circular vortices is to reduce the computational cost compared with the methods where the Biot and Savart integration is assessed by a heavy numerical integration.



Scheme 1 : local coordinate system and notations.

In the cylindrical coordinate system associated with the vortex ring of radius (a), the induced velocity vector at the point P(r, \eta, z) can be expressed as follows :

- radial component :

$$v_{ir} = \frac{a.z}{4\pi} \times \int_0^{2\pi} \frac{\gamma(\xi) \cos(\xi - \eta)}{(r^2 + a^2 + z^2 - 2ar \cos(\xi - \eta))^{3/2}} d\xi$$

- ortho-radial (or tangential) component :

$$v_{it} = \frac{a.z}{4\pi} \times \int_0^{2\pi} \frac{\gamma(\xi) \sin(\xi - \eta)}{(r^2 + a^2 + z^2 - 2ar \cos(\xi - \eta))^{3/2}} d\xi$$

- axial component :

$$v_{iz} = \frac{a^2}{4\pi} \times \int_0^{2\pi} \frac{\gamma(\xi) (1 - r/a \cos(\xi - \eta))}{(r^2 + a^2 + z^2 - 2ar \cos(\xi - \eta))^{3/2}} d\xi$$

If the vorticity distribution on the ring is approximated by a Fourier series :

$$\gamma(\xi) = \gamma_0 + \gamma_{1c} \cos(\xi) + \gamma_{1s} \sin(\xi) + \dots + \gamma_{hc} \cos(h\xi) + \gamma_{hs} \sin(h\xi) + \dots$$

the previous integrations can be decomposed into :

$$v_{ir} = \frac{a.z}{4\pi} \times \left\{ \gamma(0) \times I(1) + \sum_{h=1}^{Nh} I_A(h) \times [\gamma(2h-1) \times \cos(\eta) + \gamma(2h) \times \sin(\eta)] \right\}$$

$$v_{it} = \frac{a \cdot z}{4\pi} \times \left\{ \sum_{h=1}^{Nh} I_C(h) \times [\gamma(2h) \times \cos(\eta) - \gamma(2h-1) \times \sin(\eta)] \right\}$$

$$v_{iz} = \frac{a^2}{4\pi} \times \left\{ \gamma(0) \times \left(I(0) - \frac{r}{a} I(1) \right) + \sum_{h=1}^{Nh} \left(I_B(h) - \frac{r}{a} I_A(h) \right) \times [\gamma(2h-1) \times \cos(\eta) + \gamma(2h) \times \sin(\eta)] \right\}$$

The global integrals (I_A , I_B , I_C) depend on the harmonic number (h). They are expressed as a double sum :

$$I_A = \sum_{k=0}^{E(h/2)} (-1)^k C_h^{2k} \sum_{\beta=0}^k (-1)^\beta \frac{k!}{(k-\beta)! \beta!} I_{h-(2k-1+2\beta)}$$

$$I_B = \sum_{k=0}^{E(h/2)} (-1)^k C_h^{2k} \sum_{\beta=0}^k (-1)^\beta \frac{k!}{(k-\beta)! \beta!} I_{h-2k+2\beta}$$

$$I_C = \sum_{k=0}^{E(h/2)} (-1)^{k+2} C_h^{2k+1} \sum_{\beta=0}^{k+1} (-1)^\beta \frac{(k+1)!}{(k+1-\beta)! \beta!} I_{h-(2k-1+2\beta)}$$

The intermediate integrals $I(h)$, which appear in the previous expressions are calculated with the formula :

$$I_h = (-1/2d)^h \left[4z^2 + (a+r)^2 \right]^{h-3/2} J_{h-1} - \sum_{i=0}^{h-1} (-2d)^i C_h^i \left(2 + \frac{r}{a} + \frac{z}{a} \right)^{h-i} I_i$$

in the peculiar case where ($r=0$), that is to say when the point is on the z -axis of the local ring coordinate system :

if (h) is odd : $I_h = 0$

$$\text{if } (h) \text{ is even : } I_h = \frac{\pi \cdot h!}{(a^2 + z^2)^{3/2} \cdot 2^{h-1} \left(\frac{h}{2}! \right)^2}$$

At the last level of this breaking down decomposition, the integrals $J(h)$ are based on the elliptic integrals of the first and second kinds :

$$J_0 = \int_0^{\pi/2} \frac{d\alpha}{\sqrt{1-m\sin^2(\alpha)}}$$

$$\text{and : } J_1 = \int_0^{\pi/2} \left(\sqrt{1-m\sin^2(\alpha)} \right) d\alpha$$

then :

$$(2h-1)J_h - 2(n-1)(2-m)J_{h-1} + (2h-3)(1-m)J_{h-2} = 0$$

The complete elliptic integrals (some developments can be found in [11]) are defined as :

$$E(k) = \int_0^{\pi/2} \sqrt{1-k^2 \sin^2 \phi} \cdot d\phi$$

$$K(k) = \int_0^{\pi/2} \frac{1}{\sqrt{1-k^2 \sin^2 \phi}} \cdot d\phi$$

Particular cases :

When the point P is on the ring ($r=a$ and $z=0$), the induced velocity is supposed to be null. As said previously, when the point is within the domain of the viscous core radius, an attenuation of the induction is applied according to Scully [6].

In order to summarise, the rings are the trailing vortex elements and their induced field can be analytically formulated with their vorticity approximated by Fourier series. The advantages of such a vortex pattern is that it is both :

- sufficiently simple to allow to push the farthest the analytical resolution of the Biot and Savart integration ; therefore, the computational time is reduced in comparison with those of more realistic representations which require a numerical integration of each vortex segment influence [e.g. 5-6];
- sufficiently sophisticated to be used in the whole flight envelope, whereas the flat vortex wake approximation (introduced by Vil'dgrube [1, chap. II, p. 30-37]) is not valid at low speeds.

In the rings model the priority has been given to the dynamic representativity rather than to the keenness of the wake representation. In the present model, the geometry and the vorticity distributions evolve dynamically in function of the rotor airloads and motions. These characteristics will be useful for time simulations. But in this paper, the model will be applied for trim computations

This simple dynamic wake model for helicopter flight dynamics simulation has been implemented in the Eurocopter generic rotorcraft simulation software called HOST (Helicopter Overall Simulation Tool, [9]).

APPLICATION TO THE PITCH-UP EFFECT PREDICTION

PITCH-UP PHENOMENON

The main rotor flow on the airframe components and the tail rotor influences their airloads and so the helicopter trim state. For example, the global effect on the horizontal stabilizer is to increase the pitch moment and therefore the pitch attitude.

From a quasi - vertical position under the rotor in hover, the wake is progressively swept back when the helicopter forward speed increases. This change in the

relative position of the rotor wake and the stabilizer, produces on the curve of the pitch attitude w.r.t. to the horizontal speed, a perturbation called the "pitch - bump" (Fig. 3).

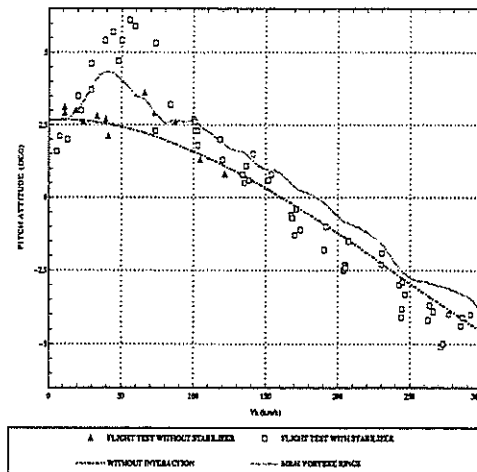


Fig. 3 : Pitch – up effect.

In [10], some flight test data with and without horizontal stabilizer, provided by EC, have been used to study this phenomenon. The measurements without horizontal tail show that the pitch-bump is mainly due to the influence of the main rotor wake on the stabilizer. The aerodynamic interferences of the wake on the other components situated behind the helicopter center of gravity (e.g. the back of the fuselage, the tail boom) contribute also to the pitch-up, but to a lesser degree. Other EC's flight tests for the aerodynamic design of the NH90 stabilizer corroborate this observation [9].

From the studies reported in [10, 12], it can be drawn that one of the most important advantages of the present model for trim calculations, is that it is sufficiently closed to the physical interaction phenomenon to give a good assessment of the airspeeds where the pitch-up effect occurs, without any adaptation of the model to trim experimental data.

However, as shown on Fig. 3, the improvement brought by the basic vortex rings model compared with the trim calculations without interaction is still insufficient. The airspeeds where the strong interference effects occur are well predicted, but the magnitude of the pitch-up is underestimated.

The following trim simulations are focused on the interaction between the main rotor wake and the horizontal tail in order to study more precisely the pitch-up effect.

MODEL CONFIGURATION

In a first step, as in these previous studies [10, 12], we choose to use the wake model only to compute the induced velocities on the stabilizer. The main rotor inflow is calculated with an other model.

* Number of rings :

- The number of groups of rings defining the length of the wake is determined as the number giving a downwash on the stabilizer very closed to the asymptotic value corresponding to an infinite wake. This study to configure the model showed that 40 groups of rings along the wake are enough.

N.B. : Of course this number would have been lower with a law to take into account the decrease of the vorticity due to viscous effects.

- The number of rings radially distributed depends on the number of blade elements. Here, we use 7 blade profiled sections. Therefore, when we want to represent all the wake (the tip and root vortices and the internal wake), 8 radial rings are used.

Usually for the computation of the interference effects, the representation of the vorticity distribution on each ring is limited to the first harmonic.

* Bound and shed vortices :

The induced velocities on the stabilizer have been computed respectively with :

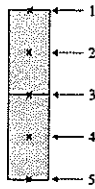
- the vortex rings model (trailing vortices),
- the trailing and shed vortices,
- the complete model, that is to say with in addition also the bound vortices.

From these comparisons [12], it can be drawn the following points :

- the influence of the bound vortices is negligible in terms of induced velocities on the rear elements which are too far from the blades,
- the effect of the shed vortices is a little more sensitive on the sidewash. Nearly null in hover, this contribution increases with the forward speed, since it comes from the azimuthal variations of the blade circulation. On the longitudinal and vertical components, their influence can be neglected.

From the flight dynamics point of view, these results confirm that for the computation of the main rotor wake influence on the horizontal tail, the trailing vortices induce the most important contribution. The influences of the bound and shed vortices may be neglected, and this will be all the more legitimate when the considered forward speed will be low.

Finally, the reference model configuration used here to calculate the interactions, will be a rotor wake represented with 40 groups of 8 vortex rings charged with a first harmonic vorticity distribution. The equilibrium state of the comprehensive helicopter model is computed through an iterative trim process from hover up to 300 km/h (or 150 km/h) with a 5 km/h step on the forward speed. The 3D induced velocities on the horizontal tail are calculated at five points regularly spaced along its span.



Scheme 2 : Location of the 5 points on the stabilizer.

EFFECT OF THE MAIN ROTOR INFLOW

In order to evaluate the influence of the rotor inflow modelling, we implemented in the HOST simulation code the model presented in [13]. Blake and White proposed an inflow model with a stronger longitudinal gradient (v_{ilc}) compared with those given by Coleman [14], Meijer-Drees [15] or Pitt and Peters [16].

This simple model corresponds to the Glauert's approximation, where the downwash is described in the wind-axis by a mean inflow (v_{i0}) and a longitudinal gradient (v_{ilc}) :

$$v_i(r, \psi) = v_{i0} + v_{ilc} \frac{r}{R} \cos(\psi)$$

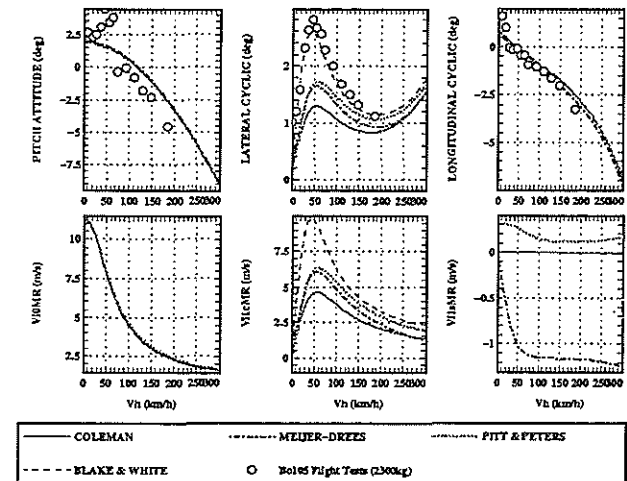
As in the other mentioned models, the mean inflow is determined by the momentum theory. The first harmonic component comes from the fore-aft variation of the downwash calculated with a horse-shoe vortex. This classical vortex system associated with the rotor disc consists of one bound vortex and two lateral trailing vortices. The linear approximation of the longitudinal velocity distribution induced by this horse-shoe vortex leads to :

$$v_{ilc} = v_{i0} \times \sqrt{2} \times \sin(\chi)$$

The term ($\sin\chi$) is introduced in order to account for the fact that (v_{ilc}) is null in hover. The horse-shoe vortex

is assumed to rotate around the rotor lateral axis with the wake skew angle (in hover or vertical flight : $\chi=0$ deg).

With this model, the variation of the lateral cyclic at



intermediate speeds is stronger than with the other models currently used in flight mechanics (Fig. 4).

Fig. 4 : Trims results with different inflow models without wake interactions (Bo105).

This simple model improves the correlation with the measurement of the lateral control due to a stronger variation of the longitudinal inflow gradient. Hence it could be expected that the effect on the stabilizer will be higher.

But, when these different rotor inflow models, are associated with the vortex rings model to compute the induced velocities on the horizontal tail, the pitch up effects are almost identical (Fig. 5).

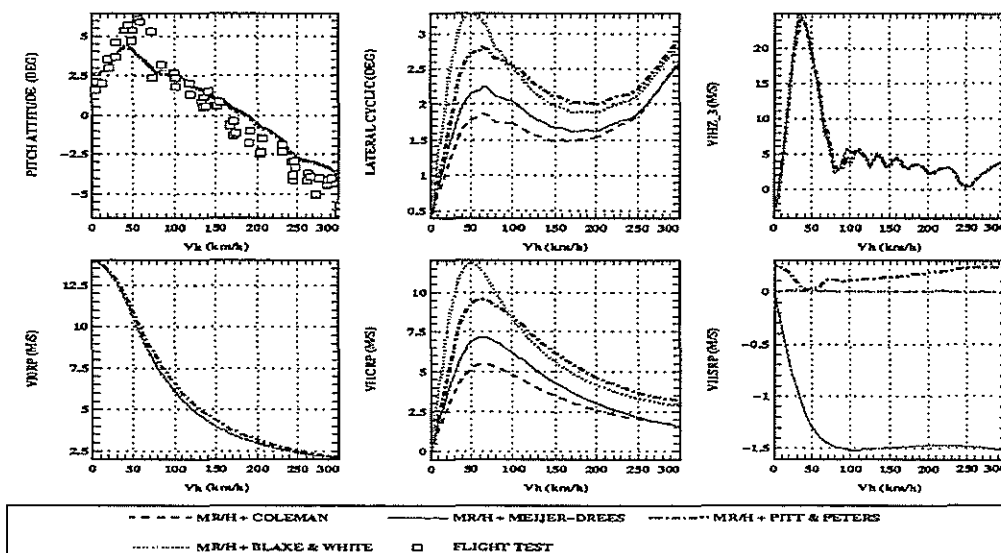


Fig. 5 : Trims results with different inflow models and with wake rings influence on the stabilizer.

The fact of changing the main rotor model has produced no effect on the wake itself. Indeed, the geometry is only affected by (v_{i0}) through the helical thread (dH) and the skew angle. The vorticity could be changed by the downwash at the rotor level. But, during the equilibrium process, the four controls and the pitch and bank angles are trimmed in order to make null the 6 accelerations of the helicopter. The stronger longitudinal inflow gradient produced by the Blake and White model, is compensated by the change of the cyclic pitch (Fig. 4-5). Thus the angles of attack are unchanged and therefore also the local blade element lifts. Hence the distribution of the circulation on the rotor remains quasi-identical, which leads to the same vortex strengths.

An other way to ensure the coupling between the main rotor inflow and the wake model, is to calculate it with the rotor wake model in a closed-loop. The iterative process to find the equilibrium of the rotor induced velocity field within the trim process of the whole helicopter is more sensitive and requires a higher computational time. Indeed, the wake model must be more refined, compared with the case in which it is only used to compute the influence on few points on the stabilizer. Moreover the computation of the wake effect on the horizontal tail can be made with only the vortex rings charged with a vorticity distribution limited to the first harmonic. But the induced velocity field on the main rotor requires to take into account the bound and shed vortices, and probably more harmonics.

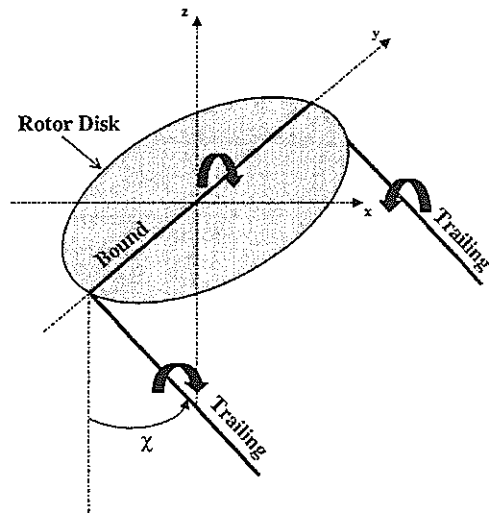
This work is still in progress. But the first results, (for which the main rotor inflow and the induced velocities on the stabilizer are calculated with the vortex rings in a closed-loop), seem to corroborate the previous conclusions. During the trim process, the change of rotor inflow is compensated by the change of controls to ensure the equilibrium, which leads to nearly the same distribution of circulation.

Therefore, the following computation will be done with the same rotor inflow model. Here we choose to use the Blake and White model [13].

EFFECT OF THE WAKE ROLL-UP

In hover or vertical flight, the wake spreads within a cylinder under the rotor. When the forward speeds increases, the wake is blown backward, but also submitted to some deformations. At high forward speed, the rotor can be viewed as a disc trailing a nearly flat wake with two lateral strong vortices as behind a wing.

In this part, the interest of modelling the wake roll-up is evaluated for the simulation of the pitch-bump. We choose to simulate this effect with a horse-shoe vortex. The two lateral branches representing the rolling-up tip vortices of the rotor disc, are skewed back with the mean-line angle (χ) of the wake as illustrated below.



Scheme 3 : Horse-Shoe Vortex (HSV) associated to the rotor disc.

An analogy between a rotor disc and a wing can be found in [17]. In this paper, the lateral distribution of circulation on the rotor disc viewed as a fixed wing is given by :

$$\Gamma = \frac{1}{(\pi\mu)} \times \Gamma_0 \left(\sqrt{1 - \bar{y}^2} - \frac{3}{2} \mu \bar{y} \ln \left[\frac{1 + \sqrt{1 - \bar{y}^2}}{|\bar{y}|} \right] \right)$$

(Γ_0) is the mean circulation on the actuator disc according to Meijer-Drees [15] :

$$\Gamma_0 = \frac{2T}{\rho \Omega \cdot R^2 \left(1 - \frac{3}{2} \mu^2 \right)}$$

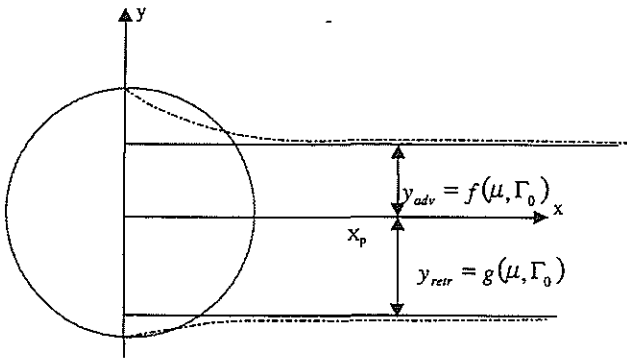
(\bar{y}) denotes the non-dimensional lateral coordinate :

$$\bar{y} = \frac{y}{R}$$

For the calculated (Γ_0, μ) at the considered flight point, the maximum of the circulation distribution ($\Gamma = f(\Gamma_0, \mu, \bar{y})$) can be determined along the span of the equivalent circular wing. The vortex strength of the two contra-rotating disc edge vortices can be taken as (Γ_{Max}), when they are fully rolled-up. The intensity of the bound vortex is (Γ_0).

In straight and steady level forward flight, the induced velocities on the horizontal tail are too low (see Fig. 6 : $v_{izMax} = 10$ m/s), and thus will not produced a significant effect on the pitch attitude. A clear reason is that the vortex lines remain too far from the calculation points. Therefore it is important to take into account the wake contraction.

If we represent the wake deformation by non-rectilinear vortex lines, we will have to perform a numerical integration of their induction. In order to still use analytical expressions, we choose to keep the right angle horse-shoe vortex representation. The lateral contraction of the two parallel trailing vortex lines, is taken into account by changing the location of their emission or attachment point on the rotor bound vortex.



Scheme 4 : Disc edge vortex lateral contraction.

These two attachment points, one on the advancing side (y_{adv}) and one on the retreating side (y_{retr}), are computed with the analytical expressions given in [17], which depend on (Γ_0, μ) and on the distance (x_{wake}) behind rotor. In our application, this latter parameter is replaced by the longitudinal coordinate of the calculation point (x_p). In fact, the curved vortex lines are represented by the rectilinear vortices which are locally at the same distances (y_{adv}, y_{retr}) to the calculation point than the deformed vortex lines (see scheme 4). This approximation is all the more valid for our application, since the wake reaches rapidly its asymptotes and because the stabilizer is not so close from the rotor center.

Of course, this model is not valid in hover or at very low speeds. In the calculation of the strength and lateral location of the disc edge vortices, some terms are divided by the advance ratio (μ) or airspeed. In [17], it is supposed that this model could be used under the classical lower limit for the flat wake theory ($\mu < 0.15$). Indeed, some results are presented for ($\mu < 0.09$). We try to apply it until hover by using (Γ_0) for the vortex strength, but it is clear that the lateral contraction model can not be applied at very low speeds. That is why, we imposed in our computations that (y_{adv}, y_{retr}) could not be lower than 0.5 (non-dimensional demi-radius of the rotor).

The induced velocities by this horse-shoe vortex model (“HSV Disc model”) at the two tips of the horizontal tail (retreating side : point 01 and advancing side : 05, see scheme 2) and at its center (point 03), are presented on Fig . 6, for each trimmed level flight from 20 km/h to 150 km/h. The 3 components are given in the helicopter airframe system (x positive forward, z downwards, and y oriented on the right).

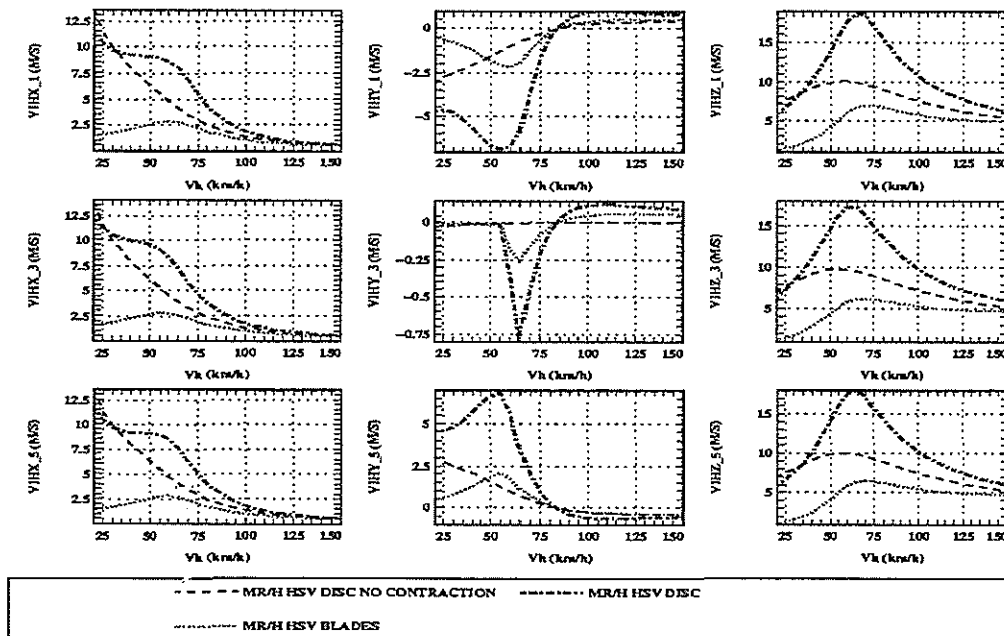


Fig. 6 : 3D induced velocities on the stabilizer.

The x-component is high at low speeds and decreases with the forward speed, since the two disc edge vortex lines are vertical in hover and rotated backward with the wake skew angle (χ). The y-component is not null at the middle station of the stabilizer (point 03) mainly because of the wake contraction, which begins here to act non-

symmetrically after 55 km/h. The combination of the helicopter pitch and bank angles introduces also a sideslip. The horse-shoe vortex system is rotated around the z-axis with this sideslip angle. Therefore, during the pitch-up phenomenon, the two lateral vortex branches do not remain at the same distance of the stabilizer middle

because of the sideslip due to the strong variations of the pitch attitude combined with those of the bank angle.

Together with the sideslip angle, the lateral contraction contributes also to some differences between the induced velocities at each tip of the stabilizer. Indeed, due to the fact that the maximum of the circulation is not located at the middle of the rotor disc, the two rolled-up vortices are not at the same distance of the rotor center. The results presented in [17], showed calculated and measured values with : $|y_{ret}| > |y_{adv}|$. This dissymmetry depends on the location of the (Γ_{Max}) . When this maximum, is reached on the retreating side, the part of the vortex sheet between the retreating edge and the location of this maximum is smaller than the one on the advancing side. Therefore this part will roll up and reach its asymptote more quickly, than the vortex sheet on the advancing side, which is attracted toward the location of the maximum of circulation.

The most important component for the pitch-up simulation is the vertical component (V_{iHz}). Due to the rotation with the skew angle, this term reach its maximum around 65 km/h. The effect of the lateral contraction increases this maximum from 10 m/s to 18 m/s (Fig. 6).

In the previous model, the rotor is assumed to be a disc. In order to obtain a model closer to a rotor with a finite number of blades, we reinforce the coupling with the blade element model used for all the simulations presented in this paper. The strength of the two rolled-up tip vortices is taken equal to the maximum of the local blade element circulation, multiplied by the number of blades. This value is generally of the same order of those determined by an iterative process from the circulation distribution given in [17]. The lateral contraction is based on the same model, but with using the mean value of the blade elements circulations also multiplied by the number of blades to be comparable with the previous model.

With this second version of the horse-shoe vortex model ("HSV blades"), the tendencies are the same as those previously observed (Fig. 6). Yet in absolute values, the induced velocities are lower. Even with the lateral contraction, the maximum downwash on the stabilizer is around 6 m/s.

Then, we choose to associate the "HSV Disc" model with our vortex rings representation in order to simulate the wake roll-up effect. Now, it is clearly not legitimate to complete the rings model with these horse-shoe vortex without subtracting some vortex influences. Indeed, the disc edge vortices represent the parts of the vortex sheets which roll up from the two lateral tips of the rotor. Therefore, we take away the vortex rings with the greatest radius, which simulate the tip blades trailing vortices.

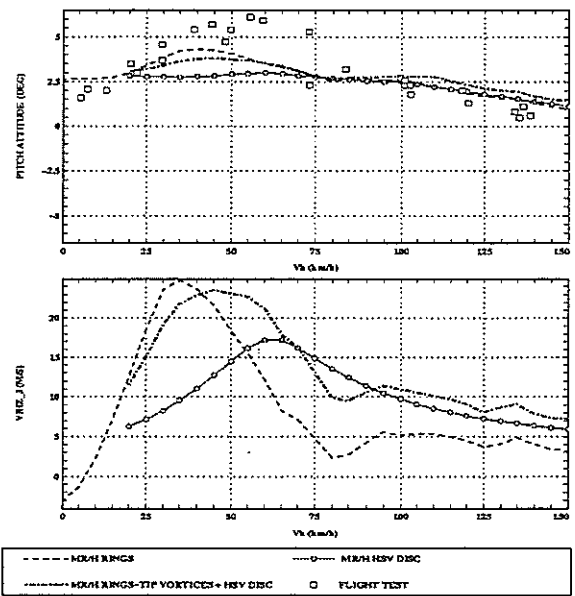


Fig. 7 : Effect of the wake-roll up : Rings model without tip vortices associated with the "HSV Disc" model.

The effects on the pitch-up behaviour are compared on (Fig. 7). Even with the lateral contraction, the downwash on the stabilizer induced by the "HSV Disc" model is too low compared with the effect of the rings model without contraction. The combination of the "HSV Disc" model with the rings model without the tip rings, induces also a lower downwash compared with the initial rings model. These results bring to the fore the importance of the tip rings, which carry the strongest vorticity. On the pitch attitude, this combination decreases the magnitude of the pitch-up and increases the pitch angle at higher speeds, which makes worse the agreement with the flight test data.

So although not legitimate, we compute these trims by combining the "HSV Disc and Blades" models with the full multi-rings model (Fig. 8). This additional downwash tends to enlarge the pitch-bump, since the "HSV model" reaches its maximum in terms of induced velocities on the stabilizer for higher forward speeds. This tendency is consistent with the fact that the wake rolls up when the forward speed increases. The highest downwash is reached at the intermediate speed corresponding to the pitch-up, because we rotate the horse-shoe vortex system with the wake skew angle. Therefore the distance between the disc edge vortices and the calculation points on the stabilizer reaches a minimum, when the mean-line of the wake goes through the horizontal tail.

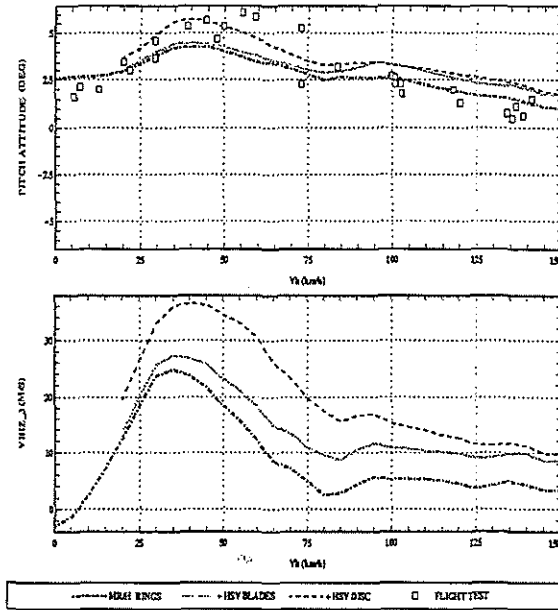


Fig. 8 : Effect of the wake-roll up : Full rings model associated with the "HSV Disc" and "HSV blades" models.

This wake-roll up effect, modeled with "HSV Blades", tends to complete the rings model at the end of the pitch-bump, where the basic rings model underestimates the downwash on the stabilizer. But it remains too low during the pitch bump and too strong at higher speeds. The combination of the "HSV Disc" with the full rings model improves significantly the pitch magnitude prediction in spite of a little overestimation at higher speeds. As mentioned, this addition is not rigorously legitimated although efficient. Therefore in the final part we preferred to go further in the refine of the rings model alone.

EFFECT OF THE WAKE CONTRACTION

In hover or vertical flight, it is also well-known that the wake is submitted to a radial contraction under the rotor. In [10, 12], we applied the radial contraction according to Landgrebe's law [18], which is based on measurements below a rotor in vertical flight conditions :

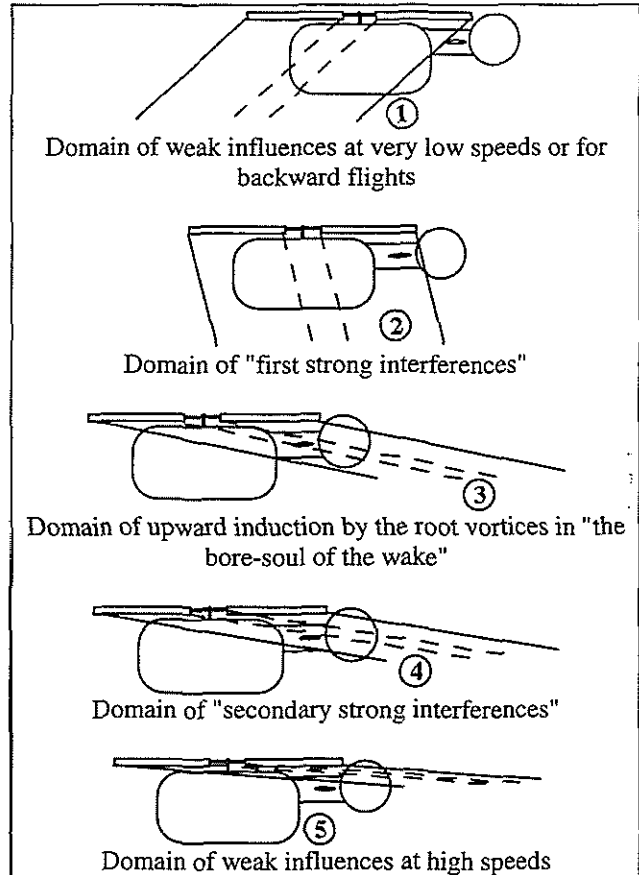
$$r_{C_{tra}}(i, \psi_{age}) = \frac{r(i_r)}{R} (\psi_{age}) = \frac{r(i_r)}{R} \times \left[r_{min} + (1 - r_{min}) \times e^{-\lambda \psi_{age}} \right]$$

with : (ψ_{age}) is the "azimuthwise age" of the vortex, and : $\lambda = 0,145 + 27 \times C_{Tae}$.

The rate of contraction proposed by Landgrebe from his measurements is : $r_{min} = 0.78$.

Here we chose not to take into account the vortices generated from the blades roots. Indeed, their vorticity is probably overestimated and since it is opposite in sign compared with the tip vortices, they induce an upwash at

the points that they surround (the stabilizer in the case 3 presented on scheme 5). These root rings are responsible of the abrupt decrease of the downwash which follows the top of the simulated pitch-bump, (for more details see [12] where we distinguished five interaction domains depending on the position of the stabilizer relative to the wake).



Scheme 5 : The five main interaction fields.

If we apply a radial contraction, this upward induction will be increased when the stabilizer will be in the case 3 of the scheme 5. Therefore the following computations are performed with 40 groups of 7 rings (root rings excluded).

The first trim results presented on Fig. 9, show the effect of a iso-radial contraction with a law based on Landgrebe's formulation which depends on the rotor thrust. The pitch-up magnitude is increased due to more density of the vortices inside the wake. With this effects on the geometry, a factor is applied on the vortex strength Fourier's coefficients $(\gamma_0, \gamma_{1c}, \gamma_{1s})$ in order to respect the conservation of the quantity :

$$\left(\oint_C \gamma \cdot dl \right)$$

For a uniform distribution, that is to say for the mean term (γ_0) , this factor is clearly equal to the ratio of the perimeters. For circular vortices this factor is :

$$C_\gamma = \frac{R_{without\ contrac.}}{R_{with\ contrac.}}$$

Here we used the strongest contraction acceptable according to the momentum theory :

$$r_{min} = \frac{\sqrt{2}}{2} = 0.707 ,$$

where (r_{min}) is the term which appears in the expression given at the beginning of this part. Hence, in that case :

$$(C_\gamma)_{max} = \frac{2}{\sqrt{2}} = 1.414$$

We choose to apply the same factor on ($\gamma_0, \gamma_{1c}, \gamma_{1s}$).

The simulation of the pitch-bump magnitude is improved, but by keeping circular vortices, the beginning of the pitch-bump occurs for higher speeds (Fig. 9). This is due to the fact that the first contact between the wake and the stabilizer is delayed in terms of forward speed, as illustrated below.

- Case without contraction :



- Case with a radial contraction :



Thus we decide to apply only a lateral contraction, in order to increase the simulated pitch-bump without changing the airspeeds area where it occurs. The wake is represented with elliptical vortices. Their longitudinal dimension (a) are unchanged compared with the initial radii of the basic rings model. Their lateral dimension (b) are submitted to a double contraction :

- one based on the momentum theory and Landgrebe's measurements, which is typical of the flow through a lifting rotor,
- the other one is based on the fixed wing theory adapted to the rotor disc in [17], which is characteristic of the lateral contraction behind an equivalent wing.

Here, we apply this second contraction only when (y_{adv}, y_{retr}) are higher than 0.5, in other words, not for the low values of (μ) for which this law is not valid. For these trim computations, the "roll-up contraction" begins to act for ($\mu=0.0125$, that is to say 10~20 km/h). The magnitude of the pitch bump and its beginning are better predicted (Fig. 9). But the combined effects of the two contractions, (and the use of $r_{min}=0.707$ instead of 0.78), lead to a too sharp increase in the downwash. This too strong effect and the end of the pitch-bump, could be better simulated with a lower contraction.

Finally, the previous non-isotropic contraction can be improved by computing a variation of the longitudinal dimension (a) with the forward speed. Indeed, it is recognised that in hover the wake is iso-radially contracted. Therefore, it is physically not correct to let unchanged the longitudinal dimension (a) of the elliptical vortices. The idea here is to apply the classical iso-radial contraction ("momentum contraction"), and then to "nip" the fluid vein laterally. By assuming that each vortex ring perimeter remains constant through the contraction, the decrease of (b) implies an increase of the longitudinal dimension (a).

So in this last step, the non-isotropic contraction of the rotor wake is performed as follows :

- on the lateral dimension (b), the same double contraction used previously is applied :
 - in hover and low speeds only the "momentum contraction" acts,
 - for higher speeds, the "roll-up contraction" is superimposed,
 - (NB.: no "roll-up contraction" is applied when one of the two terms (y_{adv}, y_{retr}) is lower than 0.5).
- on the longitudinal dimension (a) :

- in hover, the "momentum contraction" acts,
- in forward flight, (a) increases when (b) is compressed :

$$a(i_r, \psi_{age}) = \frac{r_{Circac} (i_r, \psi_{age})^2}{b(i_r, \psi_{age})}$$

(NB.: for ($\mu < 0.025$, ie. $V_H \approx 20$ km/h), (a) can not be higher than 1, ie. than the non-dimensional rotor radius).

This expression comes from the assumed conservation of the perimeter :

$$Perim_{ellipse} (a, b)(i_r, \psi_{age}) = 2\pi \cdot r_{Circac} (i_r, \psi_{age})$$

No simple analytical expression is available for the perimeter of an ellipse. Therefore we supposed that the ratio of the perimeters can be approximated by the square root of the ratio of the areas :

$$\frac{P_{circle}}{P_{ellipse}} = 1 \approx \sqrt{\frac{S_{circle}}{S_{ellipse}}}$$

thus the conservation of the perimeters is here traduced by the conservation of the surfaces of the ellipses:

$$\pi \cdot a(i_r, \psi_{age}) b(i_r, \psi_{age}) = \pi \cdot r_{Circac} (i_r, \psi_{age})^2$$

which leads to the previous formula for computing each (a).

For all elliptic contraction, we used :

$$C_\gamma = \frac{R_{without\ contrac}}{\sqrt{a \times b}}$$

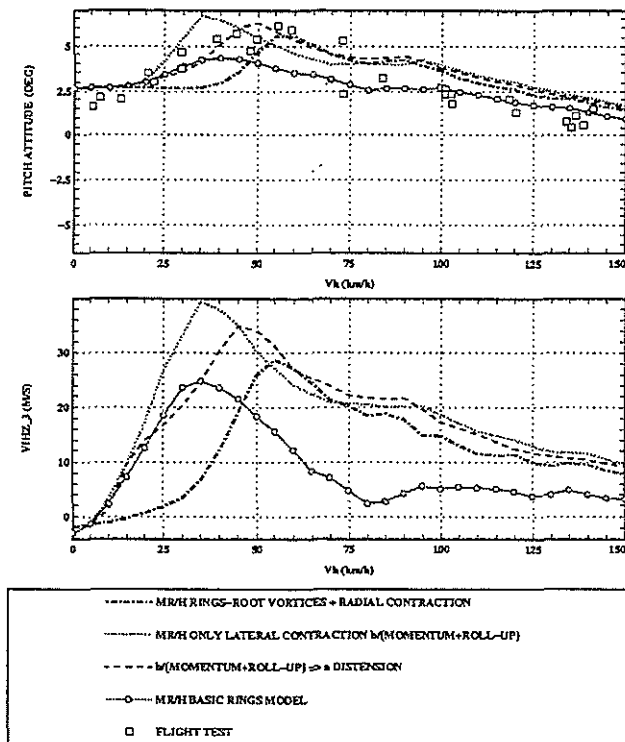


Fig. 9 : Effect of the wake contraction.

This last non-isotropic contraction provides a good prediction of the pitch-bump. The magnitude is well predicted and the overall form is in better agreement with the flight test data. Only the end of the pitch-up is a little overestimated. This is probably due to the fact that the root vortices are excluded, since the decrease in the downwash is stronger with the basic rings model near 80 km/h. Because of the same reason and of the fixed-wing contraction ("roll-up"), the pitch attitude is also slightly overestimated at higher speeds.

CONCLUSIONS

A rotor wake model has been developed by ONERA for the purposes of helicopter flight dynamics. In order to be useful both for trim computations and dynamic manoeuvres simulations, a simple geometrical form is prescribed for the trailing vortex elements (circular or elliptic). The vorticity distributions on the rings are described by Fourier series. The formulation is presented in details down to the induction expressions, which are unlimited in harmonics.

In the second part, the prediction of the pitch-up behaviour, mainly due to the main rotor wake influence on the horizontal tail, has been studied with the vortex rings model. The effects of the main rotor inflow, of the wake roll-up and of the wake contraction, have been considered.

The change of the rotor inflow model has a very little impact due to the way to trim the simulated helicopter by changing its controls and attitudes.

The simulation of the two lateral rotor disc edge vortices with a horse-shoe vortex, improves the magnitude of the predicted pitch-bump, when their effects are superimposed with those of the rings model. But this combination should be refined in order to add only the wake roll-up effect, which in fact appears mainly at higher speeds. Nevertheless, this representation of the two strong contra-rotating disc edge vortices, could also be applied to other interferences phenomena, (for instance with the tail rotor or the fin).

The most promising improvements have been obtained by modelling the wake contraction. The use of elliptic vortices allows to simulate non-isotropic contraction of the fluid vein. Some simple analytical laws have been proposed to calculate the lateral contraction and the longitudinal expansion of the wake without using the flight tests data.

ACKNOWLEDGEMENTS

This work has been supported by the French Ministry of Defence (SPAE). The authors would like to thank Eurocopter for permission to present these results.

REFERENCES

- [1] V.E. Baskin, L.S. Vil'dgrube, E.S. Vozhdayev, G.I. Maykapar :
"Theory of the lifting airscrew", N.A.S.A.-T.T.F.-823, February 1976.
- [2] X. Zhao, H.C. Curtiss:
"A linearized model of helicopter dynamics including correlation with flight test", 2nd International Conference on Rotorcraft Basic Research, College Park, 16-18 February 1988.
- [3] M. D. Takahashi :
"A flight-dynamic helicopter mathematical model with a single flap-lag-torsion main rotor", N.A.S.A. TM-102267, February 1990.
- [4] H. C. Curtiss, R. M. McKillip :
"Studies of a flat wake rotor theory", N.A.S.A. CR-190936, October 1992.
- [5] T.R. Quackenbush, D. B. Bliss :
"Free wake prediction of rotor flow fields for interactional aerodynamics", 44th Annual Forum of the A.H.S., June 1988.
- [6] W. Johnson :
"A Comprehensive Analytical Model of Rotorcraft Aerodynamics and Dynamics, Part I : Analysis and Development", N.A.S.A. TM-81182, June 1980.

- [7] **P.-M. Basset :**
"Contributions to the improvement of a simulation model of helicopter flight mechanics",
 Doctoral Thesis of the Mediterranean University, Aix-Marseille II, Laboratoire O.N.E.R.A.-Ecole de l'Air, 29 Septembre 1995.
- [8] **P.-M. Basset, F. Tchen-Fo :**
"Study of the rotor wake distortion effects on the helicopter pitch-roll cross-coupling",
 24th European Rotorcraft Forum, Marseilles (France), September 15-17 1998.
- [9] **P. Eglin :**
"Aerodynamic Design of the NH90 Helicopter Stabilizer", 23rd E.R.F., Dresden, Germany, paper n° 68, 16-18 September 1997.
- [10] **P.-M. Basset :**
"Modeling of the Dynamic Inflow on the Main Rotor and the Tail Components in Helicopter Flight Mechanics", 22nd European Rotorcraft Forum, Brighton (U.K.), September 17-19 1996, and 53rd A.H.S. Annual Forum, Virginia Beach (US), 29/04-1/05/97.
- [11] **P. F. Bird, M. D. Friedman :**
"Handbook of elliptic integrals for engineers and scientists", Springer-Verlag University Press, 2nd edition, 1971.
- [12] **P.-M. Basset :**
"Modelling of the Main Rotor Wake Influences on the Rear Elements for the Simulation of the Helicopter Flight Dynamics",
 34th Symposium of Applied Aerodynamics, A.A.A.F., Marseilles, March 1998.
- [13] **F. White, B. B. Blake :**
"Improved Method of Predicting Helicopter Control Response and Gust Sensitivity", A.H.S. Annual Forum, May 1979.
- [14] **Coleman, R.P., Feingold, A.M., and Stempin, C.W.**, Evaluation of the induced Velocity Field of an Idealised helicopter Rotor, NACA ARR L5E10, 1945.
- [15] **Drees, J.M. Jr.**, A theory of Airflow Through Rotors and its Application to Some Helicopter Problems, J. Helicopter Assoc. Great Britain, Vol. 3, No, 2, July-Sept. 1949.
- [16] **D.A. Peters, N. Haquang :**
"Dynamic inflow for practical applications",
 J^{al} of the American Helicopter Society, T. N., vol. 33, n° 4, pp. 64-68, October 1988.
- [17] **J.P. Roos** "An analytical Model for the Determination of Disc edge Vortex Strength, Location and Geometry at Low to Intermediate Flying Speeds", 22nd European Rotorcraft Forum, Brighton (U.K.), September 17-19 1996.
- [18] **A.R.L. Bramwel**, "Helicopter dynamics", Departement of Aeronautics, the City University, London, printed by E. Arnold ltd., 1976.